Ab Initio Calculations of the Magnetic Coupling between a Ni(II) Ion and Two Nitroxide Radicals in *cis* and *trans* Positions

Nicolas Suaud, Hélène Bolvin, and Jean-Pierre Daudey*

IRSAMC, 118 Route de Narbonne, 31062 Toulouse Cedex, France

Received January 6, 1999

The magnetic couplings between a Ni(II) center in an octahedral environment and two nitroxides in its coordination sphere are calculated by *ab initio* methods. The system is well described by a Heisenberg model. Fully variational calculations (DDCI2) give results similar to those of combined variational/perturbative calculations (CASPT2), and some DFT results are obtained. The effect of some structural parameters is studied: the *cis* and *trans* positions and the angles and the distances of the nitroxides with respect to the nickel center. We show that the magnetic couplings are almost the same in the *cis* and in the *trans* complexes; thus, the only relevant geometric parameters for ferromagnetic or antiferromagnetic couplings are the orientations and the distances of the nitroxide ligands with respect to the Ni(II) center. Direct exchange between the magnetic centers is calculated: it depends neither on the angles nor on the *cis* or *trans* conformations, showing that the superexchange contribution is the only angle-dependent one.

I. Introduction

One of the challenging approaches to synthesize magnetic molecular materials is the organic−inorganic one depending on the nature of the magnetic centers. In such materials, one or several paramagnetic ligands are coordinated to a paramagnetic transition metal or lanthanide ion.[1] The two magnetic centers in such complexes are very close to one another, and this should enhance the magnitude of the magnetic couplings.

Recently, Ovcharenko *et al.*[2] synthesized a complex of Ni(II) with two nitroxide radicals in the coordination sphere (NiL_2); this complex crystallizes in two phases. In the first one, the two nitroxide ligands are in equivalent *trans* positions, while in the second one, the two nitroxides are in the *cis* position and nonequivalent; the most striking feature is that, in the first case, the coupling between the nitroxides and the nickel is antiferromagnetic, whereas in the second, there are both antiferromagnetic and ferromagnetic couplings. However, the positions of the nitroxides are different in each case (distance and orientation) (see Table 1), so it is not possible to evaluate whether there is any *cis*−*trans* effect, or if the differences in the values of the couplings are only due to the structural changes.

In this paper, we intend to discriminate between the two effects through *ab initio* calculations. The complex is modeled, and calculations are then performed, independently changing the geometrical parameters of the nitroxides with respect to the nickel. Furthermore, the value of the direct exchange is calculated, and its dependency on geometric deformations is studied.

We used a greatly simplified model for the NiL_2 complex: the goal of this study is not to reproduce the experimental data but to propose a model of the molecule which makes accurate calculations possible and which allows us to qualitatively understand the experimental data.

Table 1. Geometrical Parameters and Experimental Values of J for α-NiL_2 and β-NiL_2[a]

compound	R (Å)	θ (deg)	φ[b] (deg)	γ (deg)	J (cm^{-1})
α-NiL_2	2.206	22.8	97.0 (−83)	40.2	−138.8
β-NiL_2	2.489	26.3	−60	59.0	−230.
	2.302	25.8	−120	5.4	19.6

[a] From ref 2. The definition of angles is given in Figure 3. [b] In α-NiL_2, φ depends on which N atom of the chelating ring is chosen to be the origin. In β-NiL_2 the origin is different from that in ref 2, as defined in section II.1.

The three main features of this work are as follows. First, with a dihydronitroxide model for the nitroxide, within a given geometry, three different *ab initio* methods are used. The first two begin with a good multiconfigurational wave function believed to describe the main physical features of the molecule (CASSCF and CASCI) and take into account dynamic correlation either variationally (DDCI2) or perturbatively (CASPT2). The third method used, the DFT method, is intrinsically monodeterminantal, and the correlation effects are taken into account by the means of an adequate functional. DDCI2 is considered to be the most accurate of these methods and permits a calibration of the other two which have the advantage of being able to handle larger molecular systems. Second, with the dihydronitroxide model, the CASSCF, CASCI, and CASPT2 methods are used to evaluate the magnetic couplings in different structures, independently changing the angles, the distances, and the *cis* or *trans* positions of the nitroxides. For a given distance, the direct exchange value is also evaluated for all sets of angles and conformations. Third, the accuracy of the dihydronitroxide model is checked. CASSCF and CASCI calculations are performed on an oxyl-3-imidazoline model, closer to the experimental nitroxide.

II. Modeling the Complex

1. Chemical Modeling of the Complex. The molecule studied is the 3-imidazoline nitroxide−bis[(1-(2,2,5,5-tetra-

(1) Caneschi, A.; Gatteschi, D.; Rey, P. *Prog. Inorg. Chem.* **1991**, *39*, 331.
(2) Ovcharenko, V. I.; Romanenko, G. V.; Ikorskii, V. N.; Musin, R. N.; Sagdeev, R. Z. *Inorg. Chem.* **1994**, *33*, 3370.

10.1021/ic990014+ CCC: $18.00
Published on Web 12/09/1999

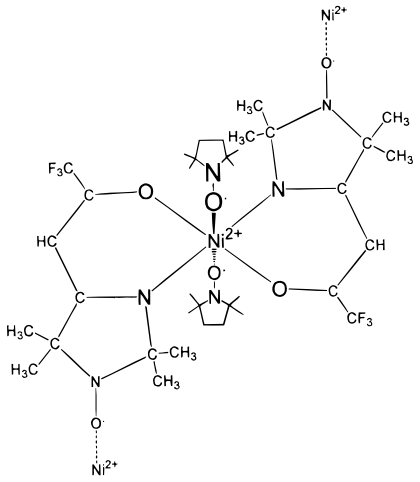

Figure 1. NiL_2 complex in the α-phase.

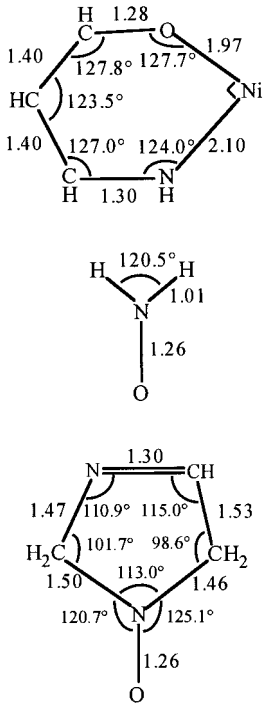

Figure 2. Structural parameters used in the *ab initio* calculations for the bidentate chain, the dihydronitroxide, and the oxyl-3-imidazoline. Distances are in angstroms.

methyl-1-oxyl-3-imidazolin-4-yl)-3′,3′,3′-trifluoro-1′-propenyl)-2′-oxy-*O*′,*N*^{3})]nickel(II) called NiL_2 (cf. Figure 1). The ligand is tridentate: one part is chelating, consisting of five atoms, and the other is bridging, ending in a nitroxide function which connects to another metal center. The magnetic portion of the ligand is well localized, and the σ system disconnects the magnetic parts of the whole molecule. In each coordination sphere of the Ni(II) ion, there are two nonmagnetic chelating ligands and two nitroxide groups which form a quasi-octahedral environment. This compound crystallizes in two different structures. In the α-NiL_2 phase, the nitroxide groups are in the *trans* position with respect to the Ni(II) ion, and in the β-NiL_2 phase, the two nitroxide groups are in the *cis* position and are not equivalent. In both cases, there is no magnetic coupling through the ligand. In the *trans* position, the fit of the experimental susceptibility gives an antiferromagnetic coupling between the nitroxides and the Ni(II) ion ($J = -138.4$ cm^{-1} assuming an Heisenberg spin Hamiltonian $\hat{H} = -J\hat{S}_A \cdot \hat{S}_B$),

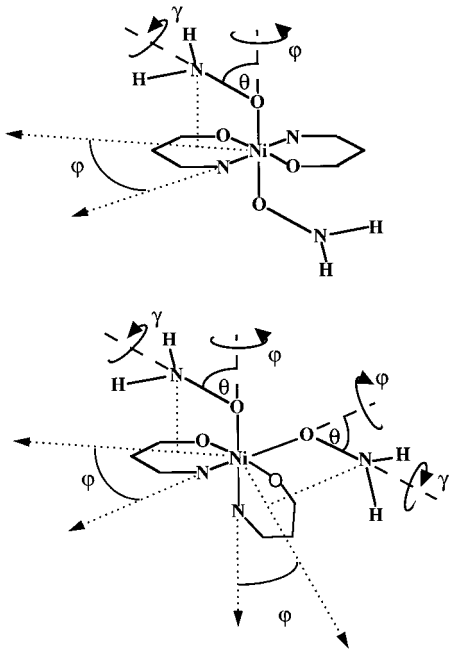

Figure 3. Angles defining the relative positions of the nickel and of the nitroxides. θ is the angle between the O−N bond of the nitroxide and the Ni−O (nitroxide) bond. γ is the rotation angle of the NH_2 plane of the nitroxide around the O−N bond of the nitroxide. $\gamma = 0°$ when NH_2 and Ni−O(nitroxide)−N(nitroxide) define the same plane. φ is the angle between the projection of the O−N(nitroxide) bond in the plane of the chelate ligand and a Ni−N(chelate) direction. In the *trans* conformation (a, top), the two chelate ligands define the same plane and both choices of origin (Ni−N(chelate) bonds) give equivalent angles. In the *cis* conformation (b, bottom), the projection is onto the chelate ligand perpendicular to the considered Ni−O(nitroxide) bond and the Ni−N(chelate) bond reference is of this chelate ligand. $\gamma = 0°$ means that the nodal plane of the π system of the nitroxide contains the Ni−O axis.

whereas in the *cis* position, there are both antiferromagnetic ($J \approx -230$ cm^{-1}) and ferromagnetic ($J \approx 19.6$ cm^{-1}) couplings.

While the coupling through the bridging ligand is by far too weak to allow 3D magnetic ordering, it makes modeling the magnetic properties of the crystal much easier. The crystal is a paramagnetic system whose magnetic domains result from the coupling among three centers: one Ni(II) ion and two nitroxides. The magnetic behavior of the nickel ion is that of a local triplet with the two unpaired electrons in the pseudo-e_g orbitals, while the magnetic behavior of the nitroxides is that of local doublets with one electron in a π^* orbital.

To be as close as possible to the real structure, one must preserve a ligand field of the same chemical nature as the real system. In our models, the nickel ion is bonded to two chelating $NH(CH)_3O$ chains and to two nitroxides. The $NH(CH)_3O$ is taken planar because the experimental bidentate chelating chain is very close to planarity. The nitroxides are first modeled by dihydronitroxides (ONH_2), and then by oxyl-3-imidazolines. Structural parameters of the latter model are those of the real chain. In all the calculations, the Ni−O(nitroxide) axis is kept perpendicular to the plane of the chelating ligand. The structural parameters used in the calculations are shown in Figure 2.

The aim of this study is to emphasize the role of the different geometrical parameters on the magnetic coupling. There are four geometrical parameters defining the position of the nitroxide: the Ni−O distance and three angles defined in Figure 3. Experimental geometries exhibit three different sets of parameters, one in the α-phase for which the two nitroxides are equivalent and two sets in the β-phase (see Table 1).

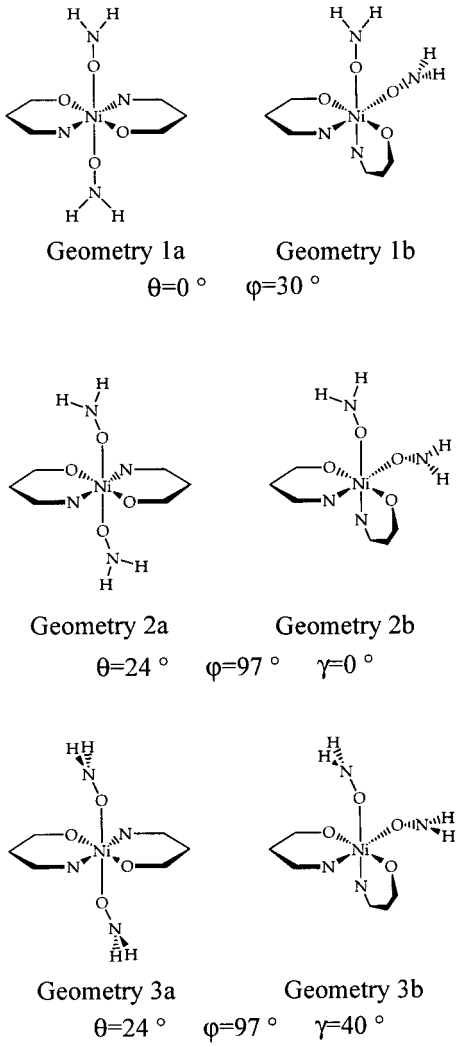

Figure 4. The six geometries used in the *ab initio* calculations (definitions of angles are those of Figure 3), presented for the dihydronitroxide radical.

We define six geometries, different from the experimental ones, to emphasize the effects of each structural parameter on the coupling.

Geometry **1a** is the most symmetrical one and transforms according to the C_{2h} group with the dihydronitroxide moiety and according to the inversion group with the imidazoline moiety (see Figure 4): the two nitroxides are in the *trans* position. The nickel atom and the oxygen and nitrogen atoms of the nitroxides are aligned ($\theta = 0°$, $\varphi = 30°$). In this geometry, the magnetic orbitals localized on the nickel are of symmetries different from those on the nitroxides.

Geometry **1b** presents the same angles as geometry **1a**, but the nitroxides are in the *cis* conformation; it transforms as C_2. Comparison of geometries **1a** and **1b** will permit us to study the *cis*−*trans* effect in the case of orthogonal magnetic orbitals.

In geometries **2a** and **2b**, θ is close to its value in the experimental systems, φ is close to that of the α-structure, and γ is close to that of the nitroxide ferromagnetically coupled to the nickel in the β-structure: $\theta = 24°$, $\varphi = 97°$, $\gamma = 0°$. **2a** has the *trans* conformation, and **2b** has the *cis* conformation. As $\gamma = 0°$, the overlap between the magnetic orbitals is tiny, even though they are of the same symmetry.

Geometries **3a** and **3b** have the γ angle of the α-structure: $\theta = 24°$, $\varphi = 97°$, $\gamma = 40°$. θ and φ are kept constant compared to those of geometries **2a** and **2b**, and the hydrogen atoms of the ONH_2 nitroxides have been rotated around the NO axis, thus changing the overlap between the magnetic orbitals. The two nitroxides are in the *trans* conformation in geometry **3a** and in the *cis* conformation in geometry **3b**. In contrast with the previous geometries, the magnetic orbitals of the nitroxides overlap with those of the Ni(II) ion, and thus a decrease of the magnetic coupling is expected.

In all the previous cases, the Ni−O distance is kept constant at 2.21 Å. Finally, we have also studied the effect of varying the Ni−O distance in geometry **1a** and of changing the nature of the nitroxide radical in geometries **1a**, **1b**, **3a**, and **3b**.

2. Heisenberg Hamiltonian for the System. The Heisenberg Hamiltonian couples the spin $S = 1$ ($\hat{\vec{S}}_{Ni}$) of the nickel ion and the two spins $S = 1/2$ of the nitroxide radicals ($\hat{\vec{S}}_{NO_A}$ and $\hat{\vec{S}}_{NO_B}$):

$$\hat{H} = -J(\hat{\vec{S}}_{Ni}\cdot\hat{\vec{S}}_{NO_A} + \hat{\vec{S}}_{Ni}\cdot\hat{\vec{S}}_{NO_B}) - j\hat{\vec{S}}_{NO_A}\cdot\hat{\vec{S}}_{NO_B}$$

J is the coupling constant between a given nitroxide and the nickel ion. In all the proposed geometries, the nitroxides are geometrically equivalent, so there is only one magnetic coupling J characterizing the two Ni−NO interactions. j is the coupling constant between the two nitroxides.

Let us call $\hat{\vec{S}}_{NO}$ the total spin of the two nitroxides and $\hat{\vec{S}}_{tot}$ the total spin of the system. The states are completely defined by the following set of quantum numbers: $|S_{Ni}; S_{NO}; S_{tot}\rangle$. One obtains four states, a singlet, $|S\rangle = |1; 1; 0\rangle$, two triplets, $|T_0\rangle = |1; 0; 1\rangle$ and $|T_1\rangle = |1; 1; 1\rangle$, and a quintet, $|Q\rangle = |1; 1; 2\rangle$. The energy gaps are

$$E_{T_0} - E_Q = J + j$$

$$E_{T_1} - E_{T_0} = J - j$$

$$E_S - E_{T_1} = J$$

For each geometry, the calculated energy levels have been fitted to this Hamiltonian. There are three energy gaps fitted with two parameters. The quality of the fit can then be evaluated by the variance defined as

$$\text{var} = \frac{[\sum_{i=1}^{N}(E^i_{ab} - E^i_{heis})^2]^{1/2}}{N}$$

where E^i_{ab} and E^i_{heis} are the ith energy gaps, calculated by the *ab initio* method and evaluated with the Heisenberg Hamiltonian, respectively, and N is the number of gaps.

III. Computational Details

1. CASSCF/CASCI Methods. The basis set used is the generally contracted ANO (atomic natural orbital) type. The starting set of primitives (17s12p9d4f) is contracted to [5s4p3d2f] for the nickel, while a (10s6p) set of primitives contracted to [3s2p] is employed for the C and N atoms and a (7s) set of primitives contracted to $[2s]^3$ for the H atoms.

In the CASSCF and CASCI calculations, performed with the MOLCAS4 package,[4] a multiconfigurational wave function is constructed for a given state, comprising all configurations obtained by distributing a given number of electrons (called active electrons) in a given number of orbitals (the active orbitals): this generates the

complete active space (CAS). In this case, the four unpaired electrons are distributed in the four "magnetic" orbitals. In the CASSCF method, configurational and orbital variational parameters are optimized in a single step, giving the minimal energy and the associated set of optimized molecular orbitals for each state required (state-specific molecular orbitals, MO1). These orbitals are symmetry-adapted. In CASCI calculations, only configurational variational parameters are optimized for a given set of orbitals, namely, the orbitals optimized for the quintet state (MO2 orbitals).

This step gives a good zeroth-order wave function which contains the main physical features but which lacks spin polarization and dynamic correlation effects. These two effects, or at least their influence on the energy differences between states with a large projection in the active space, are taken into account either variationally or perturbatively.

2. DDCI2 Method. The variational DDCI2 method (difference dedicated configuration interaction)[5−7] is implemented in the CASDI program.[8] Starting with a common set of molecular orbitals, namely, MO2, the CAS and the additional space formed by all the single and the following double excitations out of the CAS are considered. If S1 (S3) is the space of the orbitals which are doubly occupied (unoccupied) in the CASSCF calculation and n_h (n_p) the number of allowed holes (particles) in S1 (S3), the DDCI2 space contains all the configurations satisfying $n_h + n_p \leq 2$. It can be shown that at the level of second-order perturbation theory, the determinants of the DDCI2 space are the only ones contributing to the energy difference between two states differing only in their spin states (magnetic states). In geometry **1a** with dihydronitroxide, the DDCI2 space comprises 136 046 determinants for the quintet state and 207 190 determinants for the singlet state.

The 1s orbital of the C, N, and O atoms and the 1s, 2s, and 2p orbitals of the Ni atom are kept frozen in these calculations.

3. CASPT2 Method. After the CASSCF step, the correlation can be taken into account in second-order perturbation theory, with the CASPT2 method through the MOLCAS4 package.[9,10] The original definition of the Fock matrix is used,[11] and an iterative procedure is chosen. We apply this method to the two sets of orbitals: the state-specific MO1 and the orbitals optimized for the quintet state, MO2, which should permit a better cancellation of errors.

The 1s orbital of the C, N, and O atoms and the 1s, 2s, and 2p orbitals of the Ni atom are kept frozen in these calculations.

4. DFT Method. Calculations have been carried out using the Gaussian-94[12] package for the DFT, making use of the broken symmetry approach.[13]

Ab initio UHF wave functions are not spin eigenstates, but are eigenfunctions of the spin projection operator, $\hat{S}_z$. To determine the two parameters J and j, the energies of three levels are necessary. We use the three following determinants, in terms of $|M_{S_{Ni}}; M_{S_{NOA}}; M_{S_{NOB}}\rangle$, where M_S is the projection of the spin on the z axis: the quintet state, $|F\rangle = |+1; +1/2; +1/2\rangle$, a broken symmetry determinant, $|BS\rangle = |+1; -1/2; +1/2\rangle$, and an antiferromagnetic determinant, $|AF\rangle = |+1; -1/2; -1/2\rangle$.

Only the first determinant is a spin eigenfunction. As proposed by Dovesi *et al.*[14] the Ising Hamiltonian can be used as a simplification of the Heisenberg Hamiltonian:

$$\hat{H} = -J(\hat{S}_{z_{Ni}} \cdot \hat{S}_{z_{NO_A}} + \hat{S}_{z_{Ni}} \cdot \hat{S}_{z_{NO_B}}) - j\hat{S}_{z_{NO_A}} \cdot \hat{S}_{z_{NO_B}}$$

The three determinants mentioned above are eigenfunctions of this Hamiltonian with the eigenvalues $-J - j/4$, $j/4$, and $J - j/4$, which permits an evaluation of J and j. It has been shown that a better result should take into account the overlap between the magnetic orbitals.[15]

A crucial problem in DFT calculations is the choice of the functional. There exist different opinions for the best choice for the calculation of magnetic couplings. In some cases, the B3LYP functional has been shown to give results very close to experimental data[16] for magnetic couplings. This functional is built with Becke's three-parameter exchange functional[17] and the Lee−Yang−Parr correlation functional.[18] In other cases, the so-called half-and-half functional[19] gives better results than the B3LYP functional for magnetic couplings.[13] This functional mixes 50% Slater and 50% Hartree−Fock exchange and does not include any correlation. Finally, another study[20] shows that either the noncorrelated Xα functional or the VWN functional gave the best agreement with experiment. The VWN approximation to the exchange correlation potential includes the local potential of Vosko, Wilk, and Nusair.[21]

In our work, only the half-and-half and the B3LYP functionals have been applied. For practical reasons, other basis sets have been used than in the previous methods, namely, the 6-311G for all atoms.

5. Direct Exchange versus Other Contributions. Analysis of the magnetic couplings is important to understand their origin and clearly assign their variations to geometrical or chemical characteristics of the compounds.

In the case of two electrons in two orbitals, the use of perturbation theory gives a straightforward decomposition. This was done for a series of Cu(II) dimers some years ago by De Loth *et al.*[6] Following the classification proposed by Anderson,[22] these authors have expressed the magnetic couplings corresponding to different levels of perturbation theory. At zeroth order, direct exchange is obtained as the direct interaction between electrons localized in the magnetic orbitals. Superexchange is due to correlation effects, at second order, inside the valence space. Additional contributions correspond to dynamical correlation. This decomposition is not straightforward in terms of configuration interaction (CI) because the different contributions do not appear as a sum, in contrast to perturbation theory. We wish to obtain a similar decomposition by comparing the results of CIs acquired in different determinantal spaces. The equivalence of direct exchange contributions shall be obtained by a CI restricted to the space of all covalent determinants built with one electron in each magnetic orbital. Direct exchange plus superexchange contributions correspond to complete CI restricted to the complete valence space, that is, the

(3) Pierloot, K.; Dumez, B.; Widmark, P.-O.; Roos, B. O. *Theor. Chim. Acta* **1995**, *90*, 87.
(4) Andersson, K.; Fülscher, M. P.; Karlström, G.; Lindh, R.; Malqvist, P.-A.; Olsen, J.; Roos, B. O.; Sadlej, A. J.; Blomberg, M. R. A.; Siegbahn, P. E. M.; Kello, V.; Noga, J.; Urban, M.; Widmark, P.-O. *MOLCAS Version 4*; Department of Theoretical Chemistry, Chemical Center, University of Lund, P.O. Box 124, S-221 00 Lund, Sweden, 1994.
(5) Miralles, J.; Daudey, J. P.; Caballol, R. *Chem. Phys. Lett.* **1992**, *198*, 555.
(6) de Loth, P.; Cassoux P.; Daudey J. P.; Malrieu, J. P. *J. Am. Chem. Soc.* **1981**, *103*, 4007.
(7) Malrieu, J. P. *J. Chem. Phys.* **1967**, *47*, 4555.
(8) Ben Amor, N.; Maynau, D. *Chem. Phys. Lett.* **1998**, *286*, 211.
(9) Andersson, K.; Malqvist, P.-Å.; Roos, B. O.; Sadlej, A. J.; Wolinski, K. *J. Phys. Chem.* **1990**, *94*, 5483.
(10) Andersson, K.; Roos, B. O. In *Modern electron structure theory*; Yarkony, R., Ed.; Advanced Series in Physical Chemistry; World Scientific Publishing Co. Pte. Itd.: Singapore, 1995; Vol. 2, Part I:55.
(11) Andersson, K.; Malqvist, P.-Å.; Roos, B. O. *J. Chem. Phys.* **1992**, *96*, 1218.
(12) *GAUSSIAN 94*: Frisch, M. J.; Trucks, G. W.; Schlegel, H. B.; Gill, P. M. W.; Johnson, B. G.; Robb, M. A.; Cheeseman, J. R.; Keith, T. A.; Petersoon, G. A.; Montgomery, J. A.; Raghavachari, K.; Al-Laham, M. A.; Zakrzewski, V. G.; Ortiz, J. V.; Foresman, J. B.; Cioslowski, J.; Stefanov, B. B.; Nanayarkkara, A.; Challacombe, M.; Peng, C. Y.; Ayala, P. Y.; Chen, W.; Wong, M. W.; Andres, J. L.; Replogle, E. S.; Gomperts, R.; Martin, R. L.; Fox, D. J.; Binkley, J. S.; Defrees, D. J.; Baker, J.; Steward, J. J. P.; Head-Gordon, M.; Gonzalez, C.; Pople, J. A., Gaussian, Inc., Pittsburgh, PA, 1994.
(13) Noodleman, L.; Peng, C. Y.; Case, D. A.; Mouesca, J.-M. *Coord. Chem. Rev.* **1995**, *144*, 199.
(14) Dovesi, R.; Ricart, J. M.; Saunders, V. R.; Orlando, R. *J. Phys. Condens. Matter* **1995**, *7*, 7997.
(15) Caballol, R.; Castell, O.; Illas, F.; Moreira, I. de P. R.; Malrieu, J. P. *J. Phys. Chem. A* **1997**, *101*, 7860.
(16) Ruiz, E.; Alemany, P.; Alvarez, S.; Cano, J. *J. Am. Chem. Soc.* **1997**, *119*, 1297.
(17) Becke, A. D. *J. Chem. Phys.* **1993**, *98*, 5648.
(18) Lee, C.; Yang, W.; Parr, R. G. *Phys. Rev. B* **1998**, *37*, 785.
(19) Martin, R. L.; Illas, F. *Phys. Rev. Lett.* **1997**, *79*, 1539.
(20) Bencini, A.; Totti, F.; Daul, C. A.; Doklo, K.; Fantucci, P.; Barone, V. *Inorg. Chem.* **1997**, *5022*, 5030.
(21) Vosko, S. H.; Wilk, L.; Nusair, M. *Can. J. Phys.* **1980**, *58*, 1200.
(22) Anderson, P. W. *Solid State Phys.* **1963**, *14*, 99.

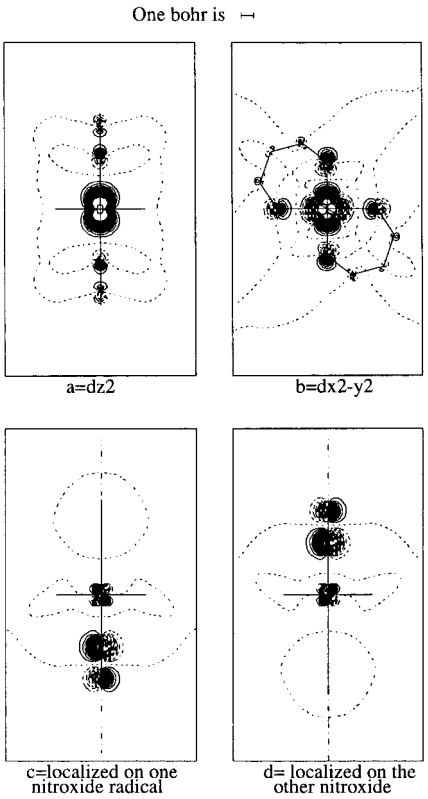

Figure 5. Magnetic orbitals with dihydronitroxide in geometry **1a**.

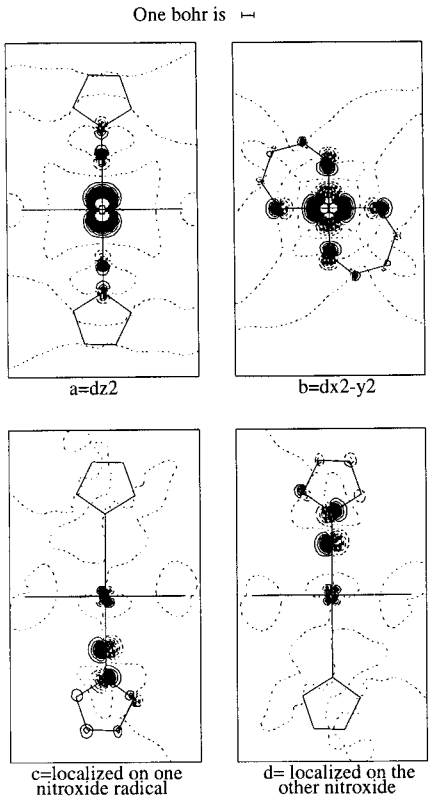

Figure 6. Magnetic orbitals with imidazoline in geometry **1a**.

Table 2. Values of J and of the Variance (cm^{-1}) Estimated with Different *ab Initio* Methods

	geometry **1a**		geometry **3a**	
method	J	var	J	var
CASSCF MO1[a]	138.0	5.3	47.3	9.6
CASCI MO2[b]	161.5	0.6	83.5	16.8
CASPT2 MO1	229.3	7.7	50.6	0.1
CASPT2 MO2	145.4	3.7	9.1	2.7
DDCI MO2	188.2	1.1	39.4	1.2
DDCI MO3[c]	183.3			
UHF[d]	201.3		117.5	
DFT[d,e]	253.2		98.5	

[a] MO1 = state-specific molecular orbitals. [b] MO2 = molecular orbitals optimized for the quintet state. [c] MO3 = molecular orbitals optimized for the singlet state. [d] Calculated with only two states. [e] Calculated with the half-and-half functional.

Table 3. Total Coupling and Direct Exchange in Different Geometries (cm^{-1})

nitroxide	geometry	K	J(CASCI)[a]	J(CASPT2)[a]
imidazoline	**1a**	146.4	145.9	
ONH_2	**1a**	161.5	161.5	145.4
ONH_2	**1b**	153.9	151.9	128.1
ONH_2	**2a**	162.9	162.9	147.0
ONH_2	**2b**	159.6	150.7	124.4
ONH_2	**3a**	165.7	83.5	9.1
ONH_2	**3b**	165.9	90.0	6.7

[a] MO2 = molecular orbitals optimized for the quintet state.

Table 4. Values of J (cm^{-1}) in Geometry **1a**, for Different Distances Ni−NO

distance (Å)	J(CASSCF)	J(CASPT2)
2.21	161.5	145.4
2.3	116.8	105.7
2.5	55.2	53.6

Table 5. Values of J (cm^{-1}) for the Two Models of Nitroxide Radicals at the CASSCF/CASCI Calculation Level

	ONH_2		imidazoline	
	CASSCF	CASCI[a]	CASSCF	CASCI[a]
geometry **1a**	+138.0	+161.5	+126.4	+145.9
geometry **1b**	+129.3	+151.9	+116.7	+135.1
geometry **3a**	+47.3	+83.5	−4.1	+30.6
geometry **3b**	+59.0	+90.0	−18.7	+12.4

[a] MO2 = molecular orbitals optimized for the quintet state.

CASSCF or CASCI results as defined in section III.1. Dynamical effects on the couplings are directly added by a CASPT2 or DDCI2 step.

There are three steps involved in the computation of the direct exchange. First, because the space generated by the determinants with one electron in one orbital is not invariant under rotation, the four symmetry-adapted magnetic orbitals must be localized. Second, the Hamiltonian matrix is written in this space and diagonalized. Finally, the magnetic coupling extracted from the energy gaps gives the direct exchange coupling.

In the first step, the four magnetic molecular orbitals obtained from CASSCF calculation (namely, the MO2 set, optimized from the quintet state) are localized. In geometry **1a** with dihydronitroxides, the two 3d magnetic orbitals of nickel belong to the A_g symmetry group ($O1_{Ni}$ and $O2_{Ni}$ orbitals) and the magnetic molecular orbitals of the nitroxides belong to the B_g and B_u symmetry groups (g and u orbitals). As the first two orbitals are already localized on the nickel, it is easy, in this case, to obtain the matrix for the transformation from delocalized CASSCF orbitals ($O1_{Ni}$, $O2_{Ni}$, g, and u) to localized orbitals (a, b, c, and d): a = $O1_{Ni}$ and b = $O2_{Ni}$ are 3d magnetic orbitals of the nickel ion, c = (g + u)/$\sqrt{2}$ and d = (g − u)/$\sqrt{2}$ are localized on the two nitroxides. The magnetic orbitals a, b, c, and d are displayed in Figures 5 and 6.

In the other geometries, as there are only two symmetry groups generated, orbitals have to be localized by numerical procedures. A procedure based on Boys' method[23] computed with the PSHF package has been used, which while not adapted to cases with two orbitals

Chart 1

$\|ab\bar{c}\bar{d}\rangle$	0					
$\|\bar{a}bc\bar{d}\rangle$	0	0				
$\|a\bar{b}c\bar{d}\rangle$	$-K_{bc}$	$-K_{ad}$	$K_{ab}+K_{cd}-K_{ac}-K_{bd}$			
$\|\bar{a}b\bar{c}d\rangle$	$-K_{bd}$	$-K_{ac}$	$-K_{cd}$	$K_{ab}+K_{cd}-K_{ad}-K_{bc}$		
$\|\bar{a}bc\bar{d}\rangle$	$-K_{ac}$	$-K_{bd}$	$-K_{ab}$	0	$K_{ab}+K_{cd}-K_{ad}-K_{bc}$	
$\|\bar{a}b\bar{c}d\rangle$	$-K_{ad}$	$-K_{bc}$	0	$-K_{ab}$	$-K_{cd}$	$K_{ab}+K_{cd}-K_{ac}-K_{bd}$

localized on the same center, did converge in most cases. Another procedure, tailored for this situation on the basis of a projection principle,[24] was carried out and gave exactly the same results.

The second step is the calculation of the exchange integrals between localized orbitals. For instance, in geometry **1a**

$$K_{ac} = K_{ad} = (K_{O1g} + K_{O1u})/2$$

$$K_{bc} = K_{bd} = (K_{O2g} + K_{O2u})/2$$

$$K_{cd} = (K_{gg} + K_{uu} - 2K_{ug})/2$$

$$K_{ab} = K_{O1O2}$$

where K_{ij} is the exchange integral between the orbitals i and j.

The Hamiltonian matrix is written as presented in Chart 1. a and b are localized on the nickel ion, while c and d are localized on each nitroxide.

The energies of the quintet, the two triplet, and the singlet states are calculated from diagonalization of this matrix and fitted with those obtained from the Heisenberg Hamiltonian as previously. Here, the J value corresponds to the direct exchange between the nitroxides and the nickel ion.

IV. Results

1. Comparison of Methods. All the methods described above have been applied to geometries **1a** and **3a**, the first one presenting a strict orthogonality of the magnetic orbitals and the second one presenting the largest overlap between these orbitals in this study. All the results are summarized in Table 2. DDCI2 will be considered as our reference.

The range of the differences between the methods is ± 50 cm^{-1}, whether or not they include dynamical correlation. This shows that it does not play a major role, as already noticed in ref 13.

For the CASCI calculations, the MO2 set of orbitals not being optimal for the triplet and singlet states, their energies are higher than in a CASSCF calculation. This choice systematically enhances ferromagnetism.

DDCI2 performed with two different sets of orbitals gave the same result.

We have applied the DFT procedure to a model compound with an $S = 1$ system (diradical CH2) coupled to two $S = 1/2$ systems (radical H), H···CH2···H. The results were very close to the full CI ones, and thus we applied this procedure to the Ni compound, but the results were less satisfactory in this case. At the UHF level, only the so-called $|F\rangle$ and $|AF\rangle$ (see section III.4) have been obtained. Different attempts to obtain the $|BS\rangle$ failed: the $S_z = 1$ states obtained were much higher in energy and had a large contribution of the spin density delocalized on the π system of the chelating ligand. The same states were obtained with the half-and-half functional, but only the $|F\rangle$ state could be obtained with the B3LYP functional. An evaluation of J was possible at the UHF level and with the half-and-half functional.

When three levels are obtained, j, the coupling between the two nitroxides, can be extracted. However, the extracted value is very small (smaller than 10 cm^{-1}), smaller than the error bar of our calculations. When this coupling is completely neglected, the same values for J are obtained and the variance of the fit is not significantly enhanced. The *ab initio* results compare very well with the proposed model Hamiltonian.

2. Structural Effects. The J values for the geometries defined in section II are summarized in Table 3. In all geometries, the coupling between the nitroxides is very small and not significant.

In geometries **3a** and **3b**, ferromagnetism is weaker than in geometries **1a**, **1b**, **2a**, and **2b**, as expected from overlap arguments. Rotating the π system along the NO axis by rotating the H atoms tunes the overlap between the magnetic π^* orbitals of the nitroxides and the magnetic 3d orbitals of the nickel. For all geometries, the *cis*−*trans* effect is small (about 10 cm^{-1}), within the range of error of the results.

The value of the direct exchange does not depend on the relative positions of the nickel and the nitroxides (angles and the *cis* or *trans* conformation). When the overlap between the magnetic orbitals is small, superexchange vanishes, so that only direct exchange contributes to the total coupling. In the case of strong overlap (geometries **3a** and **3b**), superexchange contributes to -80 cm^{-1}.

Results for the different experimental distances between the metal ion and the nitroxides are given in Table 4. J decreases exponentially with the distance.

3. Effect of the Nature of the Nitroxides. All the results are summarized in Table 5. Changing the nature of the nitroxides has a large influence on the J value when the overlap is large (geometries **3a** and **3b**). The K value depends only slightly on the nature of the nitroxides in geometry **1a**. From previous results, one can assume the K value is independent of geometry. Thus, the superexchange is about -115 cm^{-1} with imidazolines in geometry **3a**, larger than with dihydronitroxides.

Localized magnetic orbitals are shown in Figures 5 and 6. Delocalization of the π^* magnetic orbital onto the imidazoline lowers the energy of the metal−ligand charge-transfer states (only singlet and triplet states). Thus, the interactions with lower-lying states are increased, stabilizing the lowest singlet and triplet states.

V. Discussion and Conclusions

Starting from a complex of nickel(II) containing two nitroxides in its coordination sphere, we have proposed a model molecule to better understand the role of the *cis*−*trans* effect. Six geometries have been taken into account, to compare the influence of the angles and of the *cis*−*trans* effect independently.

Different methods have been compared, a variational one, DDCI2, a variational-perturbative one, CASSCF/CASPT2, and

(23) Boys, S. F. *Rev. Mod. Phys.* **1960**, *32*, 296. Foster, J. M.; Boys, S. F. *Rev. Mod. Phys.* **1960**, *32*, 300.
(24) Suaud, N.; Malrieu, J. P. Unpublished results.

DFT methods. Differences in the values obtained by these methods lie within a range of ± 50 cm^{-1}.

The angle which has the greatest influence on the coupling is the so-called γ, which is the rotation of the nitroxides along the N−O axis: actually, this angle has a great influence on the overlap between the magnetic orbitals localized on the nickel and on the nitroxides. Direct exchange is unchanged and superexchange increases strongly when γ varies from zero to 60°.

In all the studied geometries, the *cis*−*trans* effect is very small, being almost negligible.

All the *ab initio* results are well fitted with a Heisenberg Hamiltonian assuming a triplet state on the nickel. The coupling between the two nitroxides is always very small and when neglected does not significantly change the values found for the coupling *J*. The excited singlet state of the nickel has been taken into account, and the values obtained for *J* are however exactly the same. A more precise study on both the definition and the role of the local singlet of the nickel will be made in a forthcoming work.

The comparison with experiment is quite difficult. It is clear that the antiferromagnetic couplings in α-NiL_2 and in β-NiL_2 arise from a strong overlap between magnetic orbitals (γ is about 40−60°) that induces a strong superexchange. In the same way, the ferromagnetic coupling in β-NiL_2 results from a very weak overlap, but the relationship between the two antiferromagnetic couplings is not obvious. In the β-phase, the coupling is much larger, although the distance is 0.28 Å longer than in the α-phase, and all the angles are in the same range: with the results of our calculation, the coupling should decrease by a factor of 3.

Acknowledgment. We thank Jean-Paul Malrieu for many fruitful discussions. The Laboratoire de Physique Quantique is Unité Mixte de Recherche 5626 of the CNRS. Part of the calculations were performed at IDRIS/CNRS.

IC990014+